An Acad Bras Cienc (2024) 96(Suppl. 3): e20240096 DOI 10.1590/0001-3765202420240096
Anais da Academia Brasileira de Ciências | *Annals of the Brazilian Academy of Sciences*
Printed ISSN 0001-3765 I Online ISSN 1678-2690
www.scielo.br/aabc | www.fb.com/aabcjournal

CHEMICAL SCIENCES

Synthesis of TiO_2 nanoparticles by the solvothermal method and application in the catalysis of esterification reactions

LUANA A.C.S. DOMINGUES, GIOVANNI M. CARRIELLO, GUILHERME M. PEGORARO & GIOVANNI P. MAMBRINI

Abstract: TiO_2 nanoparticles have numerous applications, prompting extensive efforts to optimize their synthesis for various technologies. This study synthesized TiO_2 nanoparticles via the solvothermal method, using a chemometric approach to vary time, temperature, and concentrations of both the precursor and crystallization agent, aiming to understand these variables' effects on crystallite size. Post-synthesis, a sample underwent treatment for sulfate adsorption to alter surface properties from hydrophobic to hydrophilic. Characterization techniques included X-ray diffraction (XRD), infrared spectroscopy (FTIR), and scanning electron microscopy (SEM). The results indicated the formation of crystalline anatase phase nanoparticles, with particle sizes ranging from 25 to 38 nm and crystallite sizes from 8 to 10 nm. Sulfation was confirmed via FTIR, and SEM revealed particle agglomeration. Catalytic performance was assessed through esterification reactions, with two analyses: one comparing nanoparticles with and without surface modification, and the other examining the effects of variables like time, catalyst amount, and temperature on product formation. Sulfated samples exhibited excellent catalytic performance, achieving 60% conversion after 2 hours at 50 °C. Pure TiO2 samples also showed good conversion rates when synthesized at higher temperatures and Ti^{4+} concentrations.

Key words: catalysis, esterification, nanoparticles, TiO_2, titanium(IV) oxide.

INTRODUCTION

Titanium(IV) oxide, TiO_2, a compound widely studied in nanotechnology, is a stable material with photocatalytic properties in the UV region, being used in water purification due to its ability to degrade organic molecules, and also being applied in sensors and in solar filters due to the response of TiO_2 to UV light. A very common application of TiO_2 is in white pigments, being a material that is present in our daily lives (Gupta & Tripathi 2011, 2012, Haider et al. 2017, Vargas Urbano et al. 2011, Robby et al. 2023, Melnikova et al. 2023). TiO_2 has three crystalline phases, namely: anatase (tetragonal arrangement), rutile (tetragonal arrangement) and brookite (orthorhombic arrangement) (Rzaij & Abass 2020, Haidry et al. 2024, Kumar Patnaik & Divya 2023). These are phases with different crystalline structures and arrangement of atoms. These phases are stable at certain particle sizes. Anatase is stable in particles smaller than 11 nm, brookite in particles from 11 to 35 nm and rutile in particles larger than 35 nm (Feltrin et al. 2013, Madras et al. 2007, Levchenko et al. 2006, Istiroyah et al. 2021, Nikolaev et al. 2020). The use of catalysts in chemical reactions allows compounds to be synthesized at a higher speed and at lower temperatures, due to the lower activation energy path provided to the reaction

by the catalyst. This factor, combined with a good reaction yield, is of great interest to the industry (Yin & Alivisatos 2005, Chen & Mao 2007, Wei et al. 2015, Alves et al. 2014, Lott & Deutschmann 2023, Wang et al. 2023, Alves et al. 2021).

Metal oxide nanoparticles have a large specific surface area, which is responsible for the high adsorption performance of these nanoparticles (Monárrez-Cordero et al. 2014, Rajh et al. 2002, Gholizadeh et al. 2023, Gakis et al. 2023), hence why they are widely used as catalysts in organic reactions (Fan & Gao 2006, Gautam et al. 2020). Due to their high specific surface area, they are used in hydrolysis and esterification reactions, in which the performance of nanoparticles is associated with the presence of Lewis acid sites characteristic of their surfaces (Alves et al. 2014, Chen et al. 2023). Gold nanoparticles supported by metal oxides, such as TiO_2, are also described as catalysts for oxidative esterification reactions (Wei et al. 2015, Farah et al. 2023, Mu et al. 2024). TiO_2 is a very stable material, tending only to agglomerate due to its high surface energy, leading to some researchers using surface modification to counteract this issue, such as using surfactants (Sun et al. 2024, Alsheheri 2021, Qamar et al. 2023).

The solvothermal method involves a precursor, a solvent and heat treatment. With the use of organic solvents, it is possible to carry out the synthesis at higher temperatures, which accelerates the crystallization process, or even allows using precursor reagents that would otherwise react with water, such as alkoxides. The solvothermal method also allows for very homogeneous shape and size distribution of nanoparticles. A specific case of this synthesis, which was used in this work, involves an organometallic precursor and a solvent, while a surfactant may or may not be used. The precursor solution, containing the substances described previously, receives heat treatment and the reaction occurs continuously under heating until precipitation of nanoparticles is observed (Yin & Alivisatos 2005, Chen & Mao 2007, Riporto et al. 2024, Kløve et al. 2024, Zhang et al. 2023).

In heterogeneous catalysis, the catalyst and reactants are in different phases, and what favors catalysis in this case is the surface of the catalyst, as it acts through covalent interactions or adsorption, making it easier to separate the final products (Yin & Alivisatos 2005, Lott & Deutschmann 2023, Gupta et al. 2020, Chen et al. 2023). Some homogeneous catalysts are used in industry, such as sodium hydroxide, in the case of biodiesel production from transesterification reactions, which can generate major environmental problems, in addition to the unwanted formation of soap. Therefore, the use of heterogeneous catalysts is better in this regard (Shi & Li 2014, Melchiorre et al. 2021, Mandari & Devarai 2022, Maquirriain et al. 2021).

Nanoparticles are effective in heterogeneous chemical catalysis, since by obtaining a material with a very small particle size of the order of nanometers, a large ratio of exposed surface per mass of catalyst is also obtained, thus improving the catalytic activity compared to the same material on larger scales. It is important to highlight that, for these nanoparticles to perform well in catalytic activity, it is necessary to have a controlled shape and size distribution, aiming for homogeneity of the material so that it can then be analyzed and applied as catalysts for reactions (Raimondi et al. 2005, Munnik et al. 2015, Campelo et al. 2009, Liu & Corma 2023, Hirschbiegel et al. 2023).

Inorganic oxides are studied for catalysis of esterification reactions due to their acidic characteristics (Endalew et al. 2011, Borges & Díaz 2012, Otroshchenko et al. 2021, Abdullah et al. 2022, Kore et al. 2021, Han et al. 2020, Wang et al.

2022). Heterogeneous acid catalysts are of great interest because they do not cause problems, such as corrosion, which can occur with the use of homogeneous catalysts (Sajjadnejad et al. 2024). Therefore, the use of solid oxides becomes a good option. Furthermore, the use of homogeneous catalysts creates greater difficulty in separating them after use (Davies et al. 2001, Thomas & Raja 2006, Sani et al. 2014, Vilcocq et al. 2014, Carriello et al. 2023). When used as a heterogeneous catalyst, TiO_2 can readily be recovered as it does not mix in the same phase as the reagents and is not consumed in the reaction, reducing negative impacts such as generating acidic or basic residues (Gupta et al. 2020).

Esterification reactions are very important for the world economy, due to organic esters having the most diverse applications, from solvents and lubricants to cosmetics and foods. A currently widely studied type of reaction is the esterification of fatty acids with alcohols to produce biodiesel. Its synthesis involves a carboxylic acid and an alcohol, which react through condensation (Alves et al. 2014, Endalew et al. 2011, Borges & Díaz 2012, Sani et al. 2014, Carriello et al. 2023, Nascimento et al. 2012, Ghedini et al. 2021, Khan et al. 2021).

The use of TiO_2 nanoparticles can overcome these problems for some reasons, such as: TiO_2 nanoparticles have acidic characteristics; TiO_2 is a stable and non-toxic inorganic oxide; its nanoparticles are solid and have a large specific surface area, which favors catalysis (Chen & Mao 2007, Al Taee & Al Shabander 2022, Mohammadi & Isazadeh 2019, Qiang et al. 2023, Rahman et al. 2023, Kowalkińska et al. 2023).

In this work, TiO_2 nanoparticles were synthesized using the solvothermal route with benzyl alcohol as a solvent, investigating through a chemometric approach the influence of variables such as reaction time, temperature, and concentrations of titanium and hydrochloric acid in the formation of nanoparticles and their agglomeration. These nanoparticles were applied as catalysts for the esterification of oleic acid with ethanol, calculating the conversion rates of the reactions by using a calibration curve and the FTIR spectra of the products, leading to a simple and non-destructive method of determining the amount of formed product.

MATERIALS AND METHODS

Titanium(IV) oxide

Synthesis

The solvothermal route was used for the synthesis of the nanoparticles, using benzyl alcohol as a solvent, titanium(IV) isopropoxide as the Ti precursor and hydrochloric acid as a crystallizing agent (Bian et al. 2016). The experiments were organized using a 2^{4-1} factorial design, whose variables and conditions are shown in Tables I and II. The levels of the variables were chosen arbitrarily.

First, 20.0 mL of benzyl alcohol (98%, Synth, Brazil) were heated until reaching the desired synthesis temperature of 100 or 150 °C. Subsequently, titanium(IV) isopropoxide (97%, Sigma Aldrich, United States of America) and hydrochloric acid (37%, Synth, Brazil) were added, and the mixture was kept under heating for Δt, according to Tables I and II. After the solvothermal treatment, the suspension was centrifuged, and the nanoparticles were washed with tetrahydrofuran (99%, Synth, Brazil) three times. TiO_2 crystallization occurs at very high temperatures, and the use of HCl as a crystallization agent allows TiO_2 crystallization at lower temperatures, below 100 °C (Watson et al. 2004). Furthermore, the surface of the nanoparticles was modified through the sulfation of TiO_2 by treatment in H_2SO_4 to verify

Table I. Variables for the synthesis of titanium(IV) oxide nanoparticles.

Variable	Lowest value (-)	Highest value (+)
$[Ti^{4+}]$	0.456 mol L^{-1}	0.912 mol L^{-1}
[HCl]	500 ppm	1000 ppm
T	100 °C	150 °C
Δt	6 h	12 h

-: Lowest value.
+: Highest value.
$[Ti^{4+}]$: Titanium isopropoxide concentration.
[HCl]: Hydrochloric acid concentration.
T: Temperature.
Δt: Reaction time.

Table II. 2^{4-1} factorial planning.

Experiment	$[Ti^{4+}]$	[HCl]	T	Δt
Ti-1	-	-	-	-
Ti-2	+	-	-	+
Ti-3	-	+	-	+
Ti-4	+	+	-	-
Ti-5	-	-	+	+
Ti-6	+	-	+	-
Ti-7	-	+	+	-
Ti-8	+	+	+	+

-: Lowest value.
+: Highest value.
$[Ti^{4+}]$: Titanium isopropoxide concentration.
[HCl]: Hydrochloric acid concentration.
T: Temperature.
Δt: Reaction time.

whether the sulfate was adsorbed on its surface. For this, a solution of 10.0 mL of 1.0 mol L^{-1} H_2SO_4 was prepared and added to a beaker. Then, 0.1 g of TiO_2 from sample 1 was added and left under stirring for 1 hour at room temperature. This sulfated sample was named Ti-9.

Characterizations

For X-ray diffractometry (XRD), a Rigaku diffractometer was used, with θ-2θ varying in the range between 5 and 75°, with an angular step of 0.02° and CuKα radiation of λ = 0.15406 nm. For Fourier transform infrared spectroscopy (FTIR), a Bruker model Equinox 55 spectrometer operating in diffuse reflectance mode was used. A total of 32 scans were performed between 400 and 4000 cm^{-1} with a resolution of 4 cm^{-1}. The samples for analysis were prepared by mixing potassium bromide and the nanoparticle sample in a proportion of 100:1, approximately. Scanning electron microscopy (SEM) was done using a Zeiss Supra 35 model microscope equipped with a field emission gun, operated at 30 kV, was used. The samples were prepared by dispersing a small amount of nanoparticles in 900 µL of tetrahydrofuran until a cloudy suspension was obtained and then 20 µL of the suspension was deposited on a monocrystalline silicon plate with dimensions of approximately 0.5 x 0.5 cm.

Catalytic tests

Initially, three preliminary tests were carried out. The first with only ethanol (99,5%, Synth, Brazil) and oleic acid (90%, Sigma Aldrich, United States of America) with a proportion of 10:1. The second test was executed in the same manner with the Ti-1 catalyst, while the third used a modified catalyst (Ti-9). All of these three tests were carried out at 70 °C for one hour with stirring in beakers sealed with parafilm to reduce alcohol volatilization, with 1% in mass of catalyst in relation to oleic acid for the catalyzed reactions. The esterification reactions can be seen in Figure 1.

After the characterization of the previous preliminary tests, the absence of alcohol and ethyl oleate was observed. Another test was carried out with the presence of catalyst (Ti-1) and at a reduced temperature of 50 °C for two hours. The absence of alcohol and ethyl oleate was then observed again. With this, three final preliminary tests were carried out. The first test had oleic acid and ethanol in a proportion of 1:100, with stirring and a temperature of 50 °C for 1 hour, the second test in the same way using a catalyst (Ti-1) and the third test using modified catalyst (Ti-9). With the ethanol to oleic acid proportion of 100:1 derived from the preliminary tests, along with the maximum temperature of 50 ºC, the definitive catalytic tests were performed, with all their variables described in Table VI.

The influence of resting time on the percentage of ethyl oleate formed was also investigated, under the same conditions of test C-2. Test C-12 was analyzed immediately after the reaction, test C-13 with one day of rest and test C-14 after two days of rest. The composition of the bottom of the container with the supernatant was also evaluated, with two analyses being carried out (C-15 and C-16) under the same conditions as C-9. Fourier transform infrared spectroscopy was used to characterize and analyze the catalytic tests, according to the methodology described by Pegoraro et al. (2022). A calibration curve was obtained by preparing mixtures of oleic acid and ethyl oleate and varying their molar fraction from pure oleic acid to pure ethyl oleate in steps of 0.1 molar fraction, resulting in 11 mixtures. As the proportional amount of ethyl oleate increases in each mixture, the carbonyl peak centered on 1747 cm^{-1} in the FTIR spectra increases in area, while the carbonyl peak of oleic acid, centered on 1717 cm^{-1} in the FTIR spectra, decreases in total area. The ratios of these areas of reagent and product carbonyl peaks were plotted versus the molar fraction of ethyl oleate for each mixture, resulting in a linear relation, whose equation was used to determine the conversion rates in the catalytic tests.

RESULTS AND DISCUSSION

Synthesis

The diffractograms obtained for the eight synthesized samples are shown in Figure 2.

Figure 2 shows the presence of peaks characteristic of the anatase phase in all synthesized samples, in accordance with literature (Wetchakun & Phanichphant 2008), which coincide with the peaks in crystallographic records (JCPDS-02-0387), in

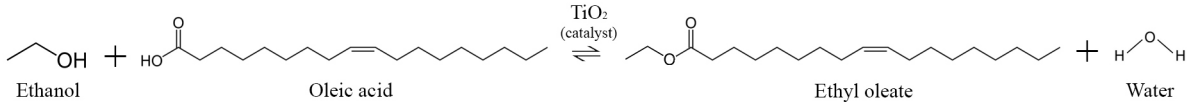

Figure 1. Scheme for the esterification of oleic acid with ethanol catalyzed by TiO_2.

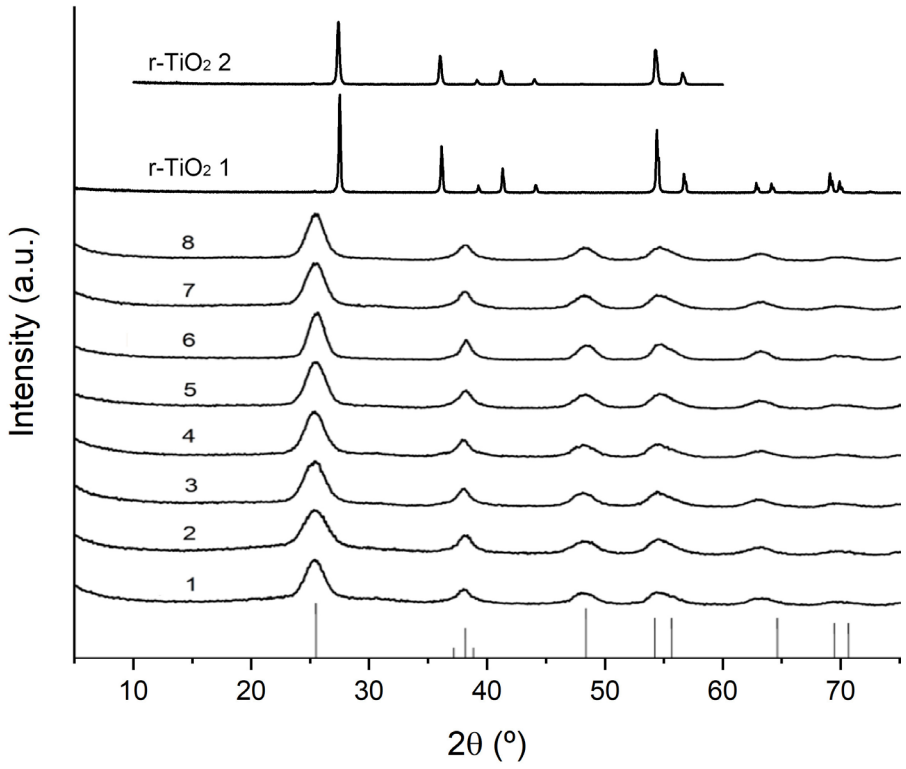

Figure 2. X-ray diffraction patterns of nanoparticle samples synthesized by the solvothermal method according to the 2^{4-1} factorial design described in Tables I and II, Ti-X, with X = 1 to 8, along with commercial TiO_2.

which well-defined peaks are characteristic of crystalline samples (Mishra 2019). All samples, even those treated for shorter periods of time and at lower temperatures, were crystalline. This result clearly shows the effectiveness of the proposed synthesis method, which allows obtaining crystalline oxides at comparatively low temperatures, in accordance with works already reported in the literature (Wetchakun & Phanichphant 2008, Bischoff & Anderson 1995, Imai & Hirashima 1999). Similar synthesis routes have already shown scalability aiming at market applications, resulting in over 20 grams of crystalline metal oxide nanoparticles in one large batch. By employing such temperatures in benzyl alcohol, the need for a calcination step is eliminated, offering cost reduction (Garnweitner et al. 2007).

Additionally, as seen in Figure 2, both commercial TiO_2 samples presented the rutile phase. The lattice parameters can be calculated using the Miller indices present in the crystallographic sheet of anatase TiO_2 (Antić et al. 2012, Pang et al. 2013). The results of Miller indices and average crystallite sizes (Dm) are shown in Table III after calculations using Bragg's Law (Bragg 1912a, b, 1913) and Scherrer equation (Miranda & Sasaki 2018).

It is observed that experiments carried out at higher temperatures of 150 °C resulted in larger crystallite size. This behavior is expected because with higher temperatures the energy within the system will be greater and more shocks will occur between particles. As nanoparticles have a very large specific surface area, there is a tendency for particles to come together after this collision, generating larger particles (Lehtinen & Zachariah 2002). There was no noticeable influence by other variables on particle size, as the first sample was satisfactory with respect to average crystallite size and lattice parameters. Therefore, this sample was

Table III. Data on the experimental conditions of the eight experiments and respective lattice parameters and average crystallite size.

Sample	$[Ti^{4+}]$	[HCl]	T	Δt	a (nm)	c (nm)	D_{m101} (nm)	D_{m200} (nm)
Ti-1	-	-	-	-	0.3794	0.9551	8.61	8.62
Ti-2	+	-	-	+	0.3790	0.9438	6.87	7.26
Ti-3	-	+	-	+	0.3798	0.9527	7.72	8.48
Ti-4	+	+	-	-	0.3794	0.9551	8.27	8.01
Ti-5	-	-	+	+	0.9403	0.9403	8.52	8.40
Ti-6	+	-	+	-	0.8733	0.8733	10.37	10.18
Ti-7	-	+	+	-	0.3790	0.9438	8.62	8.61
Ti-8	+	+	+	+	0.3786	0.9462	9.32	9.20

-: Lowest value.
+: Highest value.
$[Ti^{4+}]$: Titanium isopropoxide concentration.
[HCl]: Hydrochloric acid concentration.
T: Temperature.
Δt: Reaction time.
a: Miller index a.
c: Miller index c.
D_{m101}: Average crystallite size referring to the plane (101)
D_{m200}: Average crystallite size referring to the plane (200)

selected for subsequent tests, as it is a sample synthesized at a lower temperature, time and concentration of reagents. The Ti-9 sample, obtained by modifying the surface of the Ti-1 sample through the adsorption of sulfate by treatment in 1 mol L^{-1} sulfuric acid for 1 hour, was analyzed by FTIR, shown in Figure 3.

The most important information to be extracted from these spectra is the incorporation of sulfate on the surface of the nanoparticles, which can be verified by the appearance of the sulfate band indicated in Figure 3. Even with a shorter sulfation time than described in the literature (Srinivasan et al. 2006, Gómez et al. 2003, López et al. 2000, Murcia et al. 2015, Fadilah et al. 2023, Wijaya et al. 2023), it was possible to obtain nanoparticles with sulfate adsorbed on their surface. Hydrophilic behavior is expected from nanoparticles with sulfate adsorbed on the surface. For application in the catalysis of esterification reactions, hydrophilic nanoparticles are important for good dispersion in alcoholic medium. Furthermore, sulfated oxides may perform better in the catalysis in question (Wu et al. 2008). Little presence of bands related to organic compounds can be observed in both samples, indicating that the washing process was effective in removing residues. The presence of -OH bands may be observed in case water is adsorbed on a specific sample, as is evident in the case of Ti-4.

Scanning electron microscopy analysis allows observing aspects related to particle size and dispersion. The formation of large agglomerates by the nanoparticles was observed. In some cases, it is possible to see some dispersed particles, but they tended to agglomerate in all nine samples. Figure 4 shows the SEM images for samples Ti-1 and T-9.

Using the images of the 9 samples, an average calculation was performed by selecting five particles from each sample at a magnitude of 50.00 KX and five clusters from each sample at a magnitude of 10.00 kV. The results are seen in Table IV.

A relatively high value is observed for the average size of the nanoparticles. With the absence of surfactant, nanoparticles tend

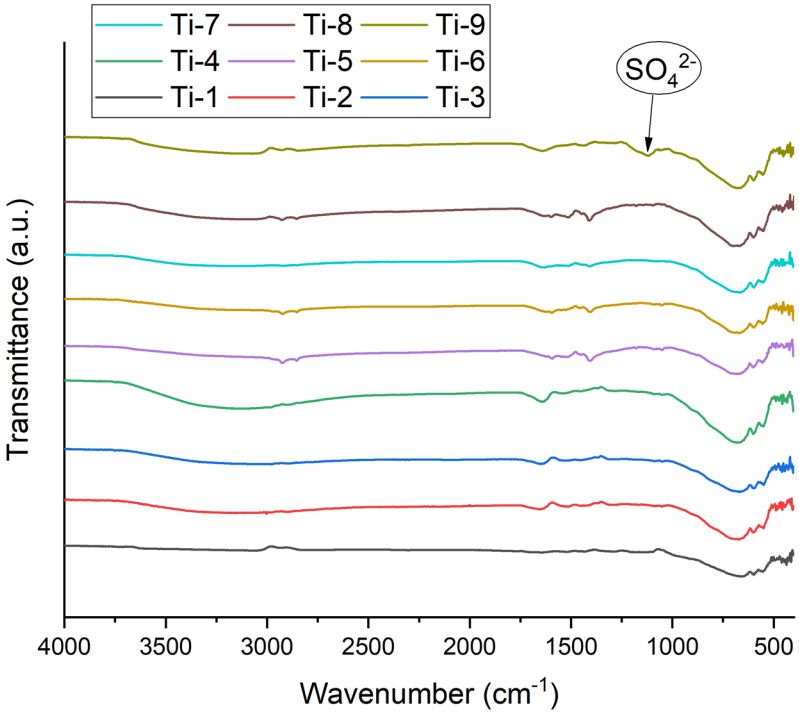

Figure 3. FTIR spectra for samples Ti-1 to Ti-9, which was treated with sulfuric acid.

to grow and agglomerate due to their high surface energy (Sanchez-Martinez et al. 2018, Santacruz-Chávez et al. 2015). Even so, it is a small and somewhat controlled size, necessary for subsequent application in catalysis of esterification reactions.

Furthermore, using the chemometric planning described in Table II and the results shown in Table IV, it is possible to calculate the primary and secondary effects of each variable on the average particle size and the average agglomerate size. The effect of each variable was calculated by subtracting the sum of the responses at the lower levels from the sum of the responses at the higher levels of that variable. The results are shown in Table V.

It can be seen in Table V that time does not significantly influence the average particle size. However, the concentration of titanium(IV) ions negatively influences the size, that is, the higher the concentration, the smaller the size of the nanoparticles. This was also observed with hydrochloric acid, but with a lesser effect. Finally, temperature has the opposite effect. The higher the temperature, the larger the average particle size.

Regarding the size of the cluster, Table V shows that the concentration of titanium(IV) ions and hydrochloric acid are negligible. Temperature has the opposite effect, the higher the temperature, the smaller the size of the cluster. Finally, time has a positive effect, since longer times resulted in larger cluster size.

The experimental observations can be justified by considering several factors. Firstly, the relatively high average size of the nanoparticles observed can be attributed to their tendency to grow and agglomerate due to their high surface energy, even without the presence of a surfactant (Chaudhuri & Paria 2011). However, this growth is somewhat controlled, resulting in a small size suitable for subsequent application in catalysis of esterification reactions. Moreover, time has a positive effect on cluster size, as longer reaction times lead to larger clusters (Stolarczyk et al. 2016, Jensen et al. 1999).

Table IV. Average particle and agglomerate size in sampling of 5 measurements.

Sample	Average particle size (nm)	Average agglomerate size (μm)
Ti-1	34.4	1.5
Ti-2	31.1	3.1
Ti-3	32.2	2.8
Ti-4	26.7	1.1
Ti-5	36.7	0.8
Ti-6	35.6	0.7
Ti-7	36.7	1.0
Ti-8	33.3	2.0
Ti-9	25.6	1.1

Table V. Primary effects on average particle size and average agglomeration size.

Variable	Effect on average particle size (nm)	Effect on average agglomerate size (nm)
$[Ti^{4+}]$	-13.3	0.87
[HCl]	-8.9	0.77
T	17.9	-4.03
Δt	-0.1	4.39

$[Ti^{4+}]$: Titanium isopropoxide concentration.
[HCl]: Hydrochloric acid concentration.
T: Temperature.
Δt: Reaction time.

Catalytic tests

The catalytic tests consisted of a study of the influence of variables such as temperature, reaction time and percentage of catalyst on the catalytic performance of the nanoparticles by quantifying the percentage of conversion of oleic acid and ethanol into ethyl oleate. The preliminary tests indicated that the temperature of 70 ºC and the proportion of 10:1 of ethanol to oleic acid were not adequate to produce ethyl oleate, leading to the evaporation of the alcohol. With a reduced temperature of 50 °C and the increase in the proportion of reagents to 100:1, the carbonyl peak of ethyl oleate was identified and the definitive catalytic tests were carried out following the variables in Table VI, in which control tests are named "B", commercial TiO_2 tests are named "T", tests catalyzed by synthesized samples are named "C" and reusability tests are called "R".

Using the methodology for quantification described previously, a conversion of 22.7% (C-1) was obtained in 1 hour of reaction and 24.1% (C-2) in two hours of reaction at 25 °C, higher than for the same experiment carried out at 50 °C. However, this sample was kept at rest before analysis, indicating that the reaction continued even without stirring.

Four other tests were carried out (C-3, C-4, C-5 and C-6) to verify whether the amount of catalyst influences the percentage of ethyl oleate formed. The experiments were carried out with an increase in temperature from 25 °C to 50 °C and with an increase in the amount of catalyst from 1% to 2%. A large increase in the percentage of ethyl oleate formed was observed,

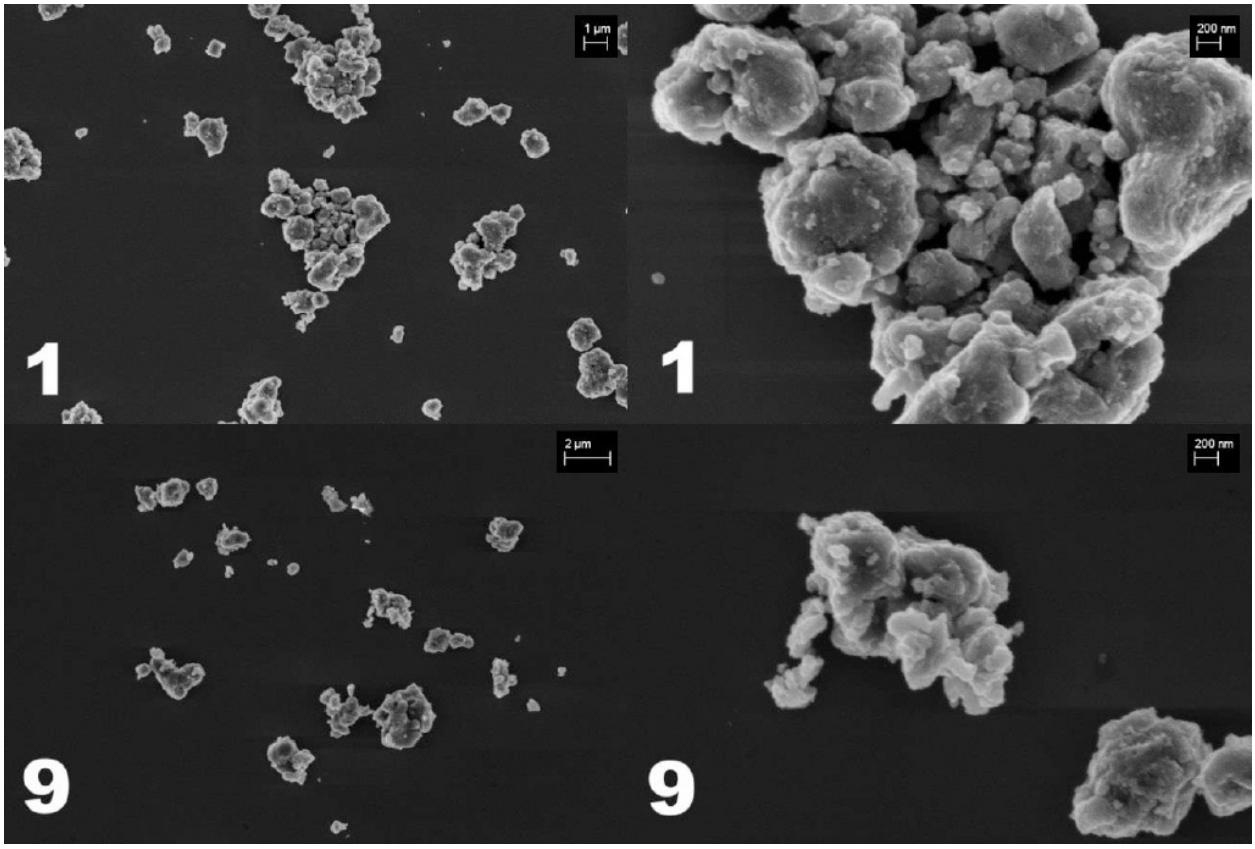

Figure 4. Scanning electron microscopy of samples Ti-1 and Ti-9.

Table VI. Catalytic test conditions and conversion percentages for all tests.

Test	Temperature (°C)	Reaction time (h)	Resting time (h)	% of catalyst	Catalyst sample	% of conversion
B-1	25	2	0	0	-	13.2
B-2	50	4	0	0	-	22.9
T-1	50	2	0	3	r-TiO_2 1	59.7
T-2	50	2	0	3	r-TiO_2 2	45.6
C-1	25	1	2	1	Ti-1	22.7
C-2	25	2	2	1	Ti-2	24.1
C-3	50	1	2	2	Ti-3	47.4
C-4	50	2	2	2	Ti-4	48.3
C-5	50	3	2	2	Ti-5	41.0
C-6	50	4	2	2	Ti-6	52.6
C-7	50	½	2	3	Ti-7	47.6
C-8	50	1	2	3	Ti-8	56.7
C-9	50	2	2	3	Ti-9	59.8
C-10	50	3	2	3	Ti-9	63.5
C-11	50	4	2	3	Ti-9	60.1
C-12	25	2	2	1	Ti-2	25.9
C-13	25	2	24	1	Ti-2	32.9
C-14	25	2	48	1	Ti-2	39.6
R-1	50	½	0	3	Ti-7	59.3
R-2	50	½	0	3	Ti-7	10.4

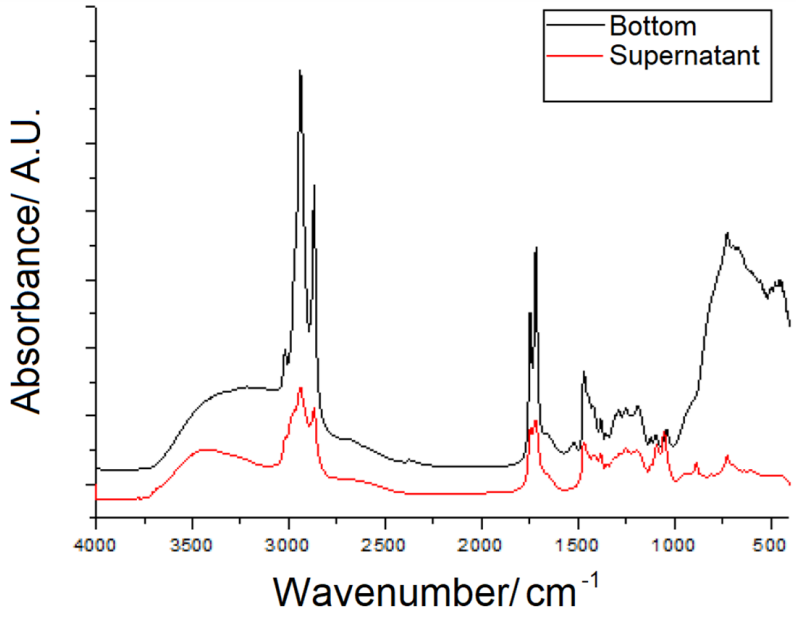

Figure 5. FTIR spectra for the C-15 and C-16 tests.

ranging from 47.4% to 52.6%, with only C-5 being an outlier at 41.0%, likely resulting from ethanol escaping the reaction vessel and leading to a smaller conversion rate. This phenomenon may have been related to both the temperature and the amount of catalyst. Therefore, five other tests were carried out (C-7, C-8, C-9, 1 C-10 and C-11), with an increase in the mass percentage of the catalyst from 2% to 3% and varied reaction times. The temperature was maintained at 50 °C and the tests were analyzed after rest. Data from all samples are shown in Table VI.

It can be seen in Table VI that the increase in the conversion rate may be associated with the increase in the amount of catalyst, given the smaller conversion rates of non-catalyzed reactions (B-1 and B-2), which is an influencing factor for the esterification reaction under the conditions that were studied. Since the surface of the catalyst is responsible for the catalytic activity (Wen et al. 2015), the results are as expected, as with a greater amount of catalyst and a larger exposed surface of the nanoparticles, the reaction has a higher conversion rate (Liu et al. 2022, Ding et al. 2017).

Comparing the conversion of the C-9 test with the commercial TiO_2 samples used under the same conditions (T-1 and T-2), a similar conversion rate was achieved with the material synthesized in this work, while the other commercial titanium oxide (T-2) did not perform as well.

Additionally, reusing the same catalyst in another catalysis reaction resulted in a lower conversion rate under the same reaction parameters, as can be seen in tests R-1 and R-2. This indicates that an additional reactivation step is required, washing the nanoparticles or even performing a calcination step (Sienkiewicz et al. 2021, Moosavi et al. 2020). These results indicate that the catalyst shows satisfactory performance only in the first cycle, with a significant reduction in catalytic activity in subsequent cycles. This can be attributed to the agglomeration of nanoparticles and the possible leaching of active sites during the recovery and reuse process (Li et al. 2010).

Analyzing tests from C-1 to C-11 in Table VI, an increase in the amount of ethyl oleate is also observed over longer reaction times, but a more

concrete conclusion cannot be established due to the reaction carrying on as the samples rest.

The C-12, C-13 and C-14 test results showed an increase in the amount of ethyl oleate over rest time, with respective conversion values of 25.9% after 2 hours of reaction time, 32.9% after one day of rest and 39.6% after two days of rest. In this way, a large amount of product is formed even after decreasing the temperature and without stirring. Over time, the nanoparticles that act as a catalyst settle on the bottom of the container, where the oily part of the solution is located.

This is in accordance with the C-15 and C-16 tests, in which it was noted that there is a presence of oleic acid and ethyl oleate both at the bottom and in the supernatant in the container. The conversion values for products in these two phases are very close, and the difference may be due to the inhomogeneity of the solution, with a certain area of the solution having a greater amount of reactants and products than another. The FTIR spectra of the products from the C-15 and C-16 tests were analyzed to obtain information about the composition in relation to other substances present, in addition to the ethyl oleate and oleic acid peaks, which are shown in Figure 5.

In the spectra of Figure 5, the presence of the absorption band referring to the OH group stretching is observed at approximately 3500 cm^{-1}. This band is characteristic of alcohols and water, and its appearance may indicate the presence of ethanol, used in the esterification reaction (Tarhan et al. 2022), or also the formation of water as a product of the reaction, in both parts of the container. The presence of ethanol together with oleic acid and a large amount of settled nanoparticles at the bottom of the container may justify the continuity of the reaction over time, which was observed in C-12, C-13 and C-14 tests. As ethanol was used in excess, it can alter the reaction equilibrium towards product formation.

This test stage provided semiquantitative results, as there were observations such as the continuity of the reaction even without heating and stirring and the composition of the supernatant and bottom of the container. For more conclusive results, it is suggested to centrifuge the catalytic test samples to remove the catalyst and heat them to evaporate the alcohol immediately after the esterification reaction. In this way, the reaction would be interrupted due to the lack of reagent and catalyst. Furthermore, the catalysts can be retrieved and further employed in other catalytic tests. Literature shows that TiO_2 catalysts can present reusability after isolation, washing and drying, while the sulfate adsorption may need to be repeated for better effectiveness, in a process called reactivation (Zhou et al. 2022, Verma et al. 2017, Berrones-Hernández et al. 2019).

CONCLUSIONS

It was possible to synthesize TiO_2 nanoparticles using the solvothermal method, obtaining a particle diameter of approximately 10 nm. It can be concluded that reaction time did not significantly influence the average particle size, and that the concentration of titanium(IV) ions and hydrochloric acid had a negative influence on it. Temperature, in turn, had a positive influence. Regarding the average size of the cluster, the concentration of titanium(IV) ions and hydrochloric acid were negligible, while temperature had a negative effect and time had a positive effect. Nanoparticles with surface modification through sulfate adsorption did not show catalytic activity, indicating that the catalyst must have been dispersed in the organic part of the solution, which was consistent with the literature, as protonation of oleic acid occurs

by the acid catalyst. The catalytic activity of TiO_2 nanoparticles was observed in the esterification reaction, and factors such as temperature and amount of catalyst influence and increase the catalytic activity of the nanoparticles. A quantity of ethyl oleate of up to 63.5% was obtained with the use of 3% catalyst at 50 °C for 3 hours. A significant decrease in catalytic activity was observed after the first cycle, indicating the need to explore methods to stabilize the catalyst. It is suggested to investigate surface modification techniques to prolong the catalyst's lifespan over multiple cycles.

Acknowledgments

This study was financed in part by the Fundação de Amparo à Pesquisa do Estado de São Paulo (FAPESP) and the Coordenação de Aperfeiçoamento de Pessoal de Nível Superior - Brasil (CAPES) - Finance Code 001.

REFERENCES

ABDULLAH FH, BAKAR NHHA & BAKAR MA. 2022. Current advancements on the fabrication, modification, and industrial application of zinc oxide as photocatalyst in the removal of organic and inorganic contaminants in aquatic systems. J Hazard Mater 424: 127416.

AL TAEE MB & AL SHABANDER BM. 2022. Study the Effect of ZnO Concentrations on The Photocatalytic Activity of TiO2/Cement Nanocomposites. Chem Methodol 6: 831-841.

ALSHEHERI SZ. 2021. Nanocomposites containing titanium dioxide for environmental remediation. Des Monomers Poly 24: 22-45.

ALVES LR, CARRIELLO GM, PEGORARO GM & FILHO JF. 2021. A utilização de óleos vegetais como fonte de polióis para a síntese de poliuretano: uma revisão. Discip Sci Nat Tecnol 22: 99-118.

ALVES MB, MEDEIROS FCM, SOUSA MH, RUBIM JC & SUAREZ PAZ. 2014. Cadmium and Tin Magnetic Nanocatalysts Useful for Biodiesel Production. J Braz Chem Soc 25: 2304-2313.

ANTIĆ Ž, KRSMANOVIĆ RM, NIKOLIĆ MG, MARINOVIĆ-CINCOVIĆ M, MITRIĆ M, POLIZZI S & DRAMIĆANIN MD. 2012. Multisite luminescence of rare earth doped TiO2 anatase nanoparticles. Mater Chem Phys 135: 1064-1069.

BERRONES-HERNÁNDEZ R, DEL CARMEN PÉREZ-LUNA Y, SÁNCHEZ-ROQUE Y, PANTOJA-ENRÍQUEZ J, GRAJALES-PENAGOS AL, LÓPEZ-CRUZ CF, LONGORIA A, EAPEN D & SEBASTIAN PJ. 2019. Heterogeneous Esterification of Waste Cooking Oil with Sulfated Titanium Dioxide (STi). Bioenerg Res 12: 653-664.

BIAN Z, ZHU J & LI H. 2016. Solvothermal alcoholysis synthesis of hierarchical TiO2 with enhanced activity in environmental and energy photocatalysis. J Photochem Photobiol 28: 72-86.

BISCHOFF BL & ANDERSON MA. 1995. Peptization Process in the Sol-Gel Preparation of Porous Anatase (TiO2). Chem Mater 7: 1772-1778.

BORGES ME & DÍAZ L. 2012. Recent developments on heterogeneous catalysts for biodiesel production by oil esterification and transesterification reactions: A review. Renew Sustain Energy Rev 16: 2839-2849.

BRAGG WH. 1912a. X-rays and Crystals. Nat 90: 219-219.

BRAGG WL. 1912b. The Specular Reflection of X-rays. Nat 90: 410-410.

BRAGG WL. 1913. The structure of some crystals as indicated by their diffraction of X-rays. Proc R Soc Lond A 89: 248-277.

CAMPELO JM, LUNA D, LUQUE R, MARINAS JM & ROMERO AA. 2009. Sustainable Preparation of Supported Metal Nanoparticles and Their Applications in Catalysis. ChemSusChem 2: 18-45.

CARRIELLO GM, PEGORARO GM, MOURATO A de S & MAMBRINI GP. 2023. Síntese de óxido de nióbio(V) dopado com lantânio e sua aplicação na reação esterificação do ácido oleico com etanol. Sci Plena 19.

CHAUDHURI RG & PARIA S. 2011. Growth kinetics of sulfur nanoparticles in aqueous surfactant solutions. J. Colloid. Interface Sci 354: 563-569.

CHEN X & MAO SS. 2007. Titanium Dioxide Nanomaterials: Synthesis, Properties, Modifications, and Applications. Chem Rev 107: 2891-2959.

CHEN Y, TANG S, LI L, LIU X & LIANG J. 2023. Selective Photocatalytic Conversion of Methane Induced by Lewis Acid-Base Pair on the Surface of In2O3/TiO2 Heterojunction Photocatalyst. ACS Sustainable Chem Eng 11: 3568-3575.

DAVIES IW, MATTY L, HUGHES DL & REIDER PJ. 2001. Are Heterogeneous Catalysts Precursors to Homogeneous Catalysts? J Am Chem Soc 123: 10139-10140.

DING Q, LI R, CHEN M & SUN M. 2017. Ag nanoparticles-TiO2 film hybrid for plasmon-exciton co-driven surface catalytic reactions. Appl Mater Today 9: 251-258.

ENDALEW AK, KIROS Y & ZANZI R. 2011. Inorganic heterogeneous catalysts for biodiesel production from vegetable oils. Biomass Bioenergy 35: 3787-3809.

FADILAH C, KURNIAWAN C, RIDWAN M, AL MUTTAQII M, AGUSTIAN E, ANDREANI AS, DWIATMOKO AA & YATI I. 2023. Synthesis of superacid sulfated TiO2 nanowires for esterification of waste cooking oil. Reac Kinet Mech Cat 136: 1529-1544.

FAN J & GAO Y. 2006. Nanoparticle-supported catalysts and catalytic reactions - a mini-review. J Exp Nanosci 1: 457-475.

FARAH J, MALLOGGI F, MISERQUE F, KIM J, GRAVEL E & DORIS E. 2023. Continuous Flow Photocatalytic Hydrogen Production from Water Synergistically Activated by TiO2, Gold Nanoparticles, and Carbon Nanotubes. Nanomaterials 13: 1184.

FELTRIN J, SARTOR MN, DE NONI JR, A BERNARDIN AM, HOTZA D & LABRINCHA JA. 2013. Superfícies fotocatalíticas de titânia em substratos cerâmicos: Parte I: Síntese, estrutura e fotoatividade. Cerâmica 59: 620-632.

GAKIS GP, AVIZIOTIS IG & CHARITIDIS CA. 2023. Metal and metal oxide nanoparticle toxicity: moving towards a more holistic structure–activity approach. Environ Sci Nano 10: 761-780.

GARNWEITNER G, GOLDENBERG LM, SAKHNO OV, ANTONIETTI M, NIEDERBERGER M & STUMPE J. 2007. Large-Scale Synthesis of Organophilic Zirconia Nanoparticles and their Application in Organic-Inorganic Nanocomposites for Efficient Volume Holography. Small 3: 1626-1632.

GAUTAM S, AGRAWAL H, THAKUR M, AKBARI A, SHARDA H, KAUR R & AMINI M. 2020. Metal oxides and metal organic frameworks for the photocatalytic degradation: A review. J Environ Chem Eng 8: 103726.

GHEDINI E, TAGHAVI S, MENEGAZZO F & SIGNORETTO M. 2021. A Review on the Efficient Catalysts for Algae Transesterification to Biodiesel. Sustain 13: 10479.

GHOLIZADEH Z, ALIANNEZHADI M, GHOMINEJAD M & TEHRANI FS. 2023. High specific surface area γ-Al2O3 nanoparticles synthesized by facile and low-cost co-precipitation method. Sci Rep 13: 6131.

GÓMEZ R, LÓPEZ T, ORTIZ-ISLAS E, NAVARRETE J, SÁNCHEZ E, TZOMPANZTZI F & BOKHIMI X. 2003. Effect of sulfation on the photoactivity of TiO2 sol–gel derived catalysts. J Mol Appl Catal A Gen 193: 217-226.

GUPTA J, AGARWAL M & DALAI AK. 2020. An overview on the recent advancements of sustainable heterogeneous catalysts and prominent continuous reactor for biodiesel production. J Ind Eng Chem 88: 58-77.

GUPTA SM & TRIPATHI M. 2011. A review of TiO2 nanoparticles. Chin Sci Bull 56: 1639-1657.

GUPTA S & TRIPATHI M. 2012. A review on the synthesis of TiO2 nanoparticles by solution route. Open Chem 10: 279-294.

HAIDER AJ, AL-ANBARI RH, KADHIM GR & SALAME CT. 2017. Exploring potential Environmental applications of TiO2 Nanoparticles. Energy Procedia 119: 332-345.

HAIDRY AA, YUCHENG W, FATIMA Q, RAZA A, ZHONG L, CHEN H, MANDEBVU CR & GHANI F. 2024. Synthesis and characterization of TiO2 nanomaterials for sensing environmental volatile compounds (VOCs): A review. Trends Anal Chem 170: 117454.

HAN X, SHENG H, YU C, WALKER TW, HUBER GW, QIU J & JIN S. 2020. Electrocatalytic Oxidation of Glycerol to Formic Acid by CuCo2O4 Spinel Oxide Nanostructure Catalysts. ACS Catal 10: 6741-6752.

HIRSCHBIEGEL C-M, ZHANG X, HUANG R, CICEK YA, FEDELI S & ROTELLO VM. 2023. Inorganic nanoparticles as scaffolds for bioorthogonal catalysts. Adv Drug Deliv Rev 195: 114730.

IMAI H & HIRASHIMA H. 1999. Preparation of Porous Anatase Coating from Sol-Gel-Derived Titanium Dioxide and Titanium Dioxide-Silica by Water-Vapor Exposure. J Am Ceram Soc 82: 2301-2304.

ISTIROYAH, ENGGE Y, MAULANA F & NURHUDA M. 2021. Literature review of the development of ZnO and TiO2 as photocatalytic material in water splitting processes. IOP Conf Ser: Earth Environ Sci 743: 012068.

JENSEN T, KELLY L, LAZARIDES A & SCHATZ GC. 1999. Electrodynamics of Noble Metal Nanoparticles and Nanoparticle Clusters. J Clust Sci 10: 295-317.

KHAN Z, JAVED F, SHAMAIR Z, HAFEEZ A, FAZAL T, ASLAM A, ZIMMERMAN WB & REHMAN F. 2021. Current developments in esterification reaction: A review on process and parameters. J Ind Eng Chem 103: 80-101.

KLØVE M, PHILIPPOT G, AUXÉMÉRY A, AYMONIER C & IVERSEN BB. 2024. Stabilizing tetragonal ZrO2 nanocrystallites in solvothermal synthesis. Nanoscale 16: 3185-3190.

KORE R, SAWANT AD & ROGERS RD. 2021. Recyclable Magnetic Fe3O4 Nanoparticle-Supported Chloroaluminate Ionic Liquids for Heterogeneous Lewis Acid Catalysis. ACS Sustain Chem Eng 9: 8797-8802.

KOWALKIŃSKA M, SIKORA K, ŁAPIŃSKI M, KARCZEWSKI J & ZIELIŃSKA-JUREK A. 2023. Non-toxic fluorine-doped TiO2 nanocrystals from TiOF2 for facet-dependent naproxen degradation. Catal. Today 413-415: 113959.

KUMAR PATNAIK R & DIVYA N. 2023. A brief review on the synthesis of TiO2 thin films and its application in dye degradation. Mater. Today Proc 72: 2749-2756.

LEHTINEN KEJ & ZACHARIAH MR. 2002. Energy accumulation in nanoparticle collision and coalescence processes. J Aerosol Sci 33: 357-368.

LEVCHENKO AA LIG, BOERIO-GOATES J, WOODFIELD BF & NAVROTSKY A. 2006. TiO2 Stability Landscape: Polymorphism, Surface Energy, and Bound Water Energetics. Chem Mater 18: 6324-6332.

LI Y, ZHANG X-D, SUN L, ZHANG J & XU H-P. 2010. Fatty acid methyl ester synthesis catalyzed by solid superacid catalyst SO42-/ZrO2-TiO2/La3+TiO2/La3+. Appl Energy 87: 156-159.

LIU L & CORMA A. 2023. Bimetallic Sites for Catalysis: From Binuclear Metal Sites to Bimetallic Nanoclusters and Nanoparticles. Chem Rev 123: 4855-4933.

LIU L, LIU P, YANG Y, DAI S, WANG Z, ZHAO A, HUANG N, CHEN J & YANG P. 2022. Dual-catalytic CuTPP/TiO2 nanoparticles for surface catalysis engineering of cardiovascular materials. Mater Today Bio 17: 100494.

LÓPEZ T, BOSCH P, TZOMPANTZI F, GÓMEZ R, NAVARRETE J, LÓPEZ-SALINAS E & LLANOS ME. 2000. Effect of sulfation methods on TiO2-SiO2 sol-gel catalyst acidity. Appl Catal A Gen 197: 107-117.

LOTT P & DEUTSCHMANN O. 2023. Heterogeneous chemical reactions—A cornerstone in emission reduction of local pollutants and greenhouse gases. Proc Combust Inst 39: 3183-3215.

MADRAS G, MCCOY BJ & NAVROTSKY A. 2007. Kinetic Model for TiO2 Polymorphic Transformation from Anatase to Rutile. J Am Ceram Soc 90: 250-255.

MANDARI V & DEVARAI SK. 2022. Biodiesel Production Using Homogeneous, Heterogeneous, and Enzyme Catalysts via Transesterification and Esterification Reactions: a Critical Review. Bioenerg Res 15: 935-961.

MAQUIRRIAIN MA, QUERINI CA & PISARELLO ML. 2021. Glycerine esterification with free fatty acids: Homogeneous catalysis. Chem Eng Res Des 171: 86-99.

MELCHIORRE M, CUCCIOLITO ME, DI SERIO M, RUFFO F, TARALLO O, TRIFUOGGI M & ESPOSITO R. 2021. Homogeneous Catalysis and Heterogeneous Recycling: A Simple Zn(II) Catalyst for Green Fatty Acid Esterification. ACS Sustainable Chem Eng 9: 6001-6011.

MELNIKOVA N, MALYGINA D, KOROKIN V, AL-AZZAWI H, ZDOROVA D, MOKSHIN E, LIYASKINA E, KURGAEVA I & REVIN V. 2023. Synthesis of Cerium Oxide Nanoparticles in a Bacterial Nanocellulose Matrix and the Study of Their Oxidizing and Reducing Properties. Mol 28: 2604.

MIRANDA MAR & SASAKI JM. 2018. The limit of application of the Scherrer equation. Acta Cryst A 74: 54-65.

MISHRA D. 2019. Studies on fly ash based geopolymeric coating material compositions incorporated with TiO 2 and Fe2O3 nanoparticles for mild steel. Indian J Chem Technol 25: 468-474.

MOHAMMADI R & ISAZADEH M. 2019. Hydrothermal and sol-gel low-temperature synthesis of tin, silver co-doped TiO2 nanoparticles with enhanced photocatalytic efficiency: artificial neural network modelling. Asian J Green Chem 3: 432-454.

MONÁRREZ-CORDERO B, AMÉZAGA-MADRID P, ANTÚNEZ-FLORES W, LEYVA-PORRAS C, PIZÁ-RUIZ P & MIKI-YOSHIDA M. 2014. Highly efficient removal of arsenic metal ions with high superficial area hollow magnetite nanoparticles synthetized by AACVD method. J Alloys Compd 586: S520-S525.

MOOSAVI S, LI RYM, LAI CW, YUSOF Y, GAN S, AKBARZADEH O, CHOWHURY ZZ, YUE X-G & JOHAN MR. 2020. Methylene Blue Dye Photocatalytic Degradation over Synthesised Fe3O4/AC/TiO2 Nano-Catalyst: Degradation and Reusability Studies. Nanomater 10: 2360.

MU X ET AL. 2024. Hollow cubic TiO2 loaded with copper and gold nanoparticles for photocatalytic CO2 reduction. J Alloys Compd 980: 173589.

MUNNIK P, DE JONGH PE & DE JONG KP. 2015. Recent Developments in the Synthesis of Supported Catalysts. Chem Rev 115: 6687-6718.

MURCIA JJ, HIDALGO MC, NAVÍO JA, ARAÑA J & DOÑA-RODRÍGUEZ JM. 2015. Study of the phenol photocatalytic degradation over TiO2 modified by sulfation, fluorination, and platinum nanoparticles photodeposition. Appl Catal B 179: 305-312.

NASCIMENTO GS, MAMBRINI GP, PARIS EC, PERES JA, COLNAGO LA & RIBEIRO C. 2012. Evaluation of the catalytic activity of oxide nanoparticles synthesized by the polymeric precursor method on biodiesel production. J Mater Res 27: 3020-3026.

NIKOLAEV AV, CHTCHELKATCHEV NM, BIBIKOV AV, SALAMATIN DA & TSVYASHCHENKO AV. 2020. Ab initio based description of the unusual increase of the electric field gradient with temperature at Ti sites in rutile TiO2. Phys Rev B 102: 174305.

OTROSHCHENKO T, JIANG G, KONDRATENKO VA, RODEMERCK U & KONDRATENKO EV. 2021. Current status and perspectives in oxidative, non-oxidative and CO2 -mediated

dehydrogenation of propane and isobutane over metal oxide catalysts. Chem Soc Rev 50: 473-527.

PANG CL, LINDSAY R & THORNTON G. 2013. Structure of Clean and Adsorbate-Covered Single-Crystal Rutile TiO2 Surfaces. Chem Rev 113: 3887-3948.

PEGORARO GM, MOURATO AS, CARRIELLO GM & MAMBRINI GP. 2022. Use of FTIR for preliminary analysis of the Conversion rate of oleic acid to ethyl oleate. Discip Sci Nat Tecnol 23: 85-97.

QAMAR OA, JAMIL F, HUSSAIN M, BAE S, INAYAT A, SHAH NS, WARIS A, AKHTER P, KWON EE & PARK Y-K. 2023. Advances in synthesis of TiO2 nanoparticles and their application to biodiesel production: A review. Chem Eng J 460: 141734.

QIANG L, ZHAO N, LIAO K, SUN X, WANG Q & JIN H. 2023. Metabolomics and transcriptomics reveal the toxic mechanism of Cd and nano TiO2 coexposure on rice (*Oryza sativa* L.). J Hazard Mater 453: 131411.

RAHMAN TU ET AL. 2023. Sustainable toxic dye removal and degradation from wastewater using novel chitosan-modified TiO2 and ZnO nanocomposites. J Mol Liq 388: 122764.

RAIMONDI F, SCHERER GG, KÖTZ R & WOKAUN A. 2005. Nanoparticles in Energy Technology: Examples from Electrochemistry and Catalysis. Angew Chem Int Ed Engl 44: 2190-2209.

RAJH T, CHEN LX, LUKAS K, LIU T, THURNAUER MC & TIEDE DM. 2002. Surface Restructuring of Nanoparticles: An Efficient Route for Ligand–Metal Oxide Crosstalk. J Phys Chem B 106: 10543-10552.

RIPORTO F ET AL. 2024. Nonclassical Nucleation and Crystallization of LiNbO3 Nanoparticles from the Aqueous Solvothermal Alkoxide Route. Small 20: 2306417.

ROBBY AFR, LALASARI LH, SOFYAN N, DHANESWARA D & YUWONO AH. 2023. A review on photocatalytic performance of TiO2 nanotubes derived from hydrothermal process. AIP Conf Proc 2538: 020001.

RZAIJ JM & ABASS AM. 2020. Review on: TiO2 Thin Film as a Metal Oxide Gas Sensor. J Chem Rev 2: 114-121.

SAJJADNEJAD M, KARKON S & HAGHSHENAS SMS. 2024. Corrosion Characteristics of Zn-TiO2 Nanocomposite Coatings Fabricated by Electro-Codeposition Process. Adv J Chem A 7: 209-226.

SANCHEZ-MARTINEZ A, CEBALLOS-SANCHEZ O, KOOP-SANTA C, LÓPEZ-MENA ER, OROZCO-GUAREÑO E & GARCÍA-GUADERRAMA M. 2018. N-doped TiO2 nanoparticles obtained by a facile coprecipitation method at low temperature. Ceram Int 44: 5273-5283.

SANI YM, DAUD WMAW & ABDUL AZIZ AR. 2014. Activity of solid acid catalysts for biodiesel production: A critical review. Appl Catal A Gen 470: 140-161.

SANTACRUZ-CHÁVEZ JA, OROS-RUIZ S, PRADO B & ZANELLA R. 2015. Photocatalytic degradation of atrazine using TiO2 superficially modified with metallic nanoparticles. J Environ Chem Eng 3: 3055-3061.

SHI W & LI J. 2014. A deactivation mechanism of sulfated titania in the esterification of acetic acid and n-butanol. Reac Kinet Mech Cat 111: 215-233.

SIENKIEWICZ A, WANAG A, KUSIAK-NEJMAN E, EKIERT E, ROKICKA-KONIECZNA P & MORAWSKI AW. 2021. Effect of calcination on the photocatalytic activity and stability of TiO2 photocatalysts modified with APTES. J Environ Chem Eng 9: 104794.

SRINIVASAN SS, WADE J, STEFANAKOS EK & GOSWAMI Y. 2006. Synergistic effects of sulfation and co-doping on the visible light photocatalysis of TiO2. J Alloys Compd 424: 322-326.

STOLARCZYK JK, DEAK A & BROUGHAM DF. 2016. Nanoparticle Clusters: Assembly and Control Over Internal Order, Current Capabilities, and Future Potential. Adv Mater 28: 5400-5424.

SUN X, WANG H, LAI Z, ZHANG Z, ZHANG Z, HANG J & SHI L. 2024. High stability, high solid content, low viscosity titanium dioxide dispersion. J Coat Technol Res 21: 1795-1804.

TARHAN İ, BAKIR MR, KALKAN O, YÖNTEM M & KARA H. 2022. Rapid determination of adulteration of clove essential oil with benzyl alcohol and ethyl acetate: Towards quality control analysis by FTIR with chemometrics. Vib Spectrosc 118: 103339.

THOMAS JM & RAJA R. 2006. The advantages and future potential of single-site heterogeneous catalysts. Top Catal 40: 3-17.

VARGAS URBANO MA, OCHOA MUÑOZ YH, ORTEGÓN FERNÁNDEZ Y, MOSQUERA P, RODRÍGUEZ PÁEZ JE & CAMARGO AMADO RJ. 2011. Nanopartículas de TiO2, fase anatasa, sintetizadas por métodos químicos. Ing Desarro 29: 186-201.

VERMA P, KAUR K, WANCHOO RK & TOOR AP. 2017. Esterification of acetic acid to methyl acetate using activated TiO2 under UV light irradiation at ambient temperature. JJ. Photochem Photobiol A Chem 336: 170-175.

VILCOCQ L, CASTILHO PC, CARVALHEIRO F & DUARTE LC. 2014. Hydrolysis of Oligosaccharides Over Solid Acid Catalysts: A Review. ChemSusChem 7: 1010-1019.

WANG L, ZHANG J, ZHANG Y, YU H, QU Y & YU J. 2022. Inorganic Metal-Oxide Photocatalyst for H2O2 Production. Small 18: 2104561.

WANG S, WAN Z, HAN Y, JIAO Y, LI Z, FU P, LI N, ZHANG A & YI W. 2023. A review on lignin waste valorization by catalytic pyrolysis: Catalyst, reaction system, and industrial symbiosis mode. J Environ Chem Eng 11: 109113.

WATSON S, BEYDOUN D, SCOTT J & AMAL R. 2004. Preparation of nanosized crystalline TiO2 particles at low temperature for photocatalysis. J Nanopart Res 6: 193-207.

WEI H, LI J, YU J, ZHENG J, SU H & WANG X. 2015. Gold nanoparticles supported on metal oxides as catalysts for the direct oxidative esterification of alcohols under mild conditions. Inorganica Chim. Acta 427: 33-40.

WEN J, LI X, LIU W, FANG Y, XIE J & XU Y. 2015. Photocatalysis fundamentals and surface modification of TiO2 nanomaterials. Chinese J Catal 36: 2049-2070.

WETCHAKUN N & PHANICHPHANT S. 2008. Effect of temperature on the degree of anatase-rutile transformation in titanium dioxide nanoparticles synthesized by the modified sol-gel method. Curr Appl Phys 8: 343-346.

WIJAYA K, HAULI L, PRABANI PF, CANDRASASI Y & FITRIAND ER. 2023. Comparative study of low-grade crude coconut oil esterification over SO4/ZrO2 and SO4/TiO2 catalysts. AIP Conf Proc 2958: 030001.

WU Z, SUN G, JIN W, HOU H, WANG S & XIN Q. 2008. Nafion® and nano-size TiO2-SO42− solid superacid composite membrane for direct methanol fuel cell. J Membr Sci 313: 336-343.

YIN Y & ALIVISATOS AP. 2005. Colloidal nanocrystal synthesis and the organic-inorganic interface. Nat 437: 664-670.

ZHANG M, CALDWELL T, HECTOR AL, GARCIA-ARAEZ N & FALVEY J. 2023. Solvothermal synthesis of nanoscale BaTiO 3 in benzyl alcohol-water mixtures and effects of manganese oxide coating to enhance the PTCR effect. Dalton Trans 52: 297-307.

ZHOU S, WU L, BAI J, LEI M, LONG M & HUANG K. 2022. Catalytic Esterification of Levulinic Acid into the Biofuel n-Butyl Levulinate over Nanosized TiO2 Particles. Nanomater 12: 3870.

How to cite

DOMINGUES LACS, CARRIELLO GM, PEGORARO GM & MAMBRINI GP. 2024. Synthesis of TiO_2 nanoparticles by the solvothermal method and application in the catalysis of esterification reactions. An Acad Bras Cienc 96: e20240096. DOI 10.1590/0001-3765202420240096.

Manuscript received on January 29, 2024;
accepted for publication on September 10, 2024

LUANA A.C.S. DOMINGUES
https://orcid.org/0009-0001-3602-3680

GIOVANNI M. CARRIELLO
https://orcid.org/0000-0003-2725-0328

GUILHERME M. PEGORARO
https://orcid.org/0000-0001-9075-7952

GIOVANNI P. MAMBRINI
https://orcid.org/0000-0001-8943-5876

Universidade Federal de São Carlos, Rodovia João Leme dos Santos, km 110, 18052-780 Sorocaba, SP, Brazil

Correspondence to: **Giovanni Miraveti Carriello**
E-mail: giovannimiraveti@estudante.ufscar.br

Author contributions

LUANA A.C.S. DOMINGUES: conducted the synthesis of TiO_2 nanoparticles and their respective characterization. GIOVANNI P. MAMBRINI: supervised the process. GIOVANNI M. CARRIELLO and GUILHERME M. PEGORARO: conducted the catalytic tests and contributed to the writing of the article.